BIBECHANA
A Multidisciplinary Journal of Science, Technology and Mathematics
ISSN 2091-0762 (online)
Journal homepage: http://nepjol.info/index.php/BIBECHANA

Hydrogen storage on platinum decorated graphene: A first-principles study

S. Lamichhane, N. Pantha, N. P. Adhikari
Central Department of Physics, Tribhuvan University
Kirtipur, Kathmandu, Nepal
E-mail : npadhikari@gmail.com, npadhikari@tucdp.edu.np
Accepted for publication: February 15, 2014

Abstract

Adsorption of gaseous/molecular hydrogen on platinum (Pt) decorated and pristine graphene have been studied systematically by using density functional theory (DFT) level of calculations implemented by Quantum ESPRESSO codes. The Perdew-Burke-Ernzerhof (PBE) type generalized gradient approximation (GGA) exchange-correlation functional and London dispersion forces have been incorporated in the DFT-D2 level of algorithm for short and long range electron-electron interactions, respectively. With reference to the binding energy of Pt on different symmetry sites of graphene supercells, the bridge (B) site has been predicted as the best adsorption site. In case of 3×3 supercell of graphene (used for detail calculations), the binding energy has been estimated as 2.02 eV. The band structure and density of states calculations of Pt adatom graphene predict changes in electronic/magnetic properties caused by the atom (Pt). The adatom (Pt) also enhances the binding energy per hydrogen molecule in Pt-graphene comparing to that in pristine graphene and records the values within the range of 1.84 eV to 0.13 eV for one to eight molecules, respectively.

Keywords: Hydrogen adsorption; DFT; Geometrical stability; Hydrogen storage; Charge transfer.

1. Introduction

Graphene, one atom thick sheet of sp^2 bonded carbon atoms arranged laterally in a honeycomb crystal lattice, has been developed from theoretical model systems [1] to experimental reality [2]. Because of the two-dimensional crystal structure, it shows many interesting properties like observable quantum Hall effect even at the room temperature [3], an ambipolar electric field effect along with ballistic conduction of charge carriers [4], tunable band gap [5] and high elasticity [6]. After the experimental production of graphene in 2004 [7], considerable research interest has been shifted to explore its unique properties and various potential applications such as in energy storage [8,9], spintronics [10] and microelectronics [11]. Various theoretical and experimental works have been performed focusing on the electronic and magnetic behaviours of different adatoms [12-15] adsorbed on graphene system, and have been found to yield many interesting results. In addition to fascinating intrinsic electronic and mechanical properties exhibited by pure graphene, the structure and properties of graphene can also be controlled and modified by adsorption and/or doping of foreign atoms [16]. Very highly porous carbon materials offer a wide variety of chemical compositions that are suitable for the adsorption and storage of gaseous molecules like hydrogen, methane and carbon dioxide. Currently, gas storage in solids is an important technology with potential applications ranging from energy, environment and all the way biology to medicine [17].

The development of the fuel cell technologies, based on hydrogen, holds the promise for producing renewable energy. The safe storage of hydrogen is also crucial for the development of hydrogen energy [18]. Carbon nanomaterials are suitable for the hydrogen storage due to high surface to volume ratio. Dillion *et al.* [19] were the first to study the hydrogen by assemblies of single walled carbon nano tubes (SWCNT) and porous activated carbon [20]. Later, many works focused on carbon based materials such as nanotubes [21,22] and fullerene C_{60} [23] have been performed. Although the transition metal atoms such as Pt and Pd, can bind multiple H_2 molecule and metal adatom carbon material can adsorb more hydrogen molecules, exceeding the minimum requirement of 6wt% for practical applications, a reliable and quantitative analysis of binding character is still insufficient. After the synthesization of graphene, its capacity of binding hydrogen molecule should be the great matter of interest.

The remaining part of the paper is organized as follows. This section (Introduction) is followed by the computational method in section 2 where we describe the systems, algorithm, and approximations for the whole calculations. The section 3 presents and discusses the results of the present work. The last section 'Conclusions and concluding remarks' highlights the summary of the paper and also presents its possible extension in near future.

2. Computational Method

The DFT based first-principles calculations [26,27] are carried out to know the structural stability and electronic properties of adatom adsorption on graphene. Further, we have studied the adsorption of hydrogen molecule/s on Pt decorated graphene to investigate its hydrogen storage capacity. The long range dispersion forces are incorporated via London interaction [28] in DFT-D2 level of approximations, implemented with the quantum ESPRESSO code [29].

The interaction between electrons and ion cores is described by ultrasoft pseudo potentials, and generalized gradient approximation (GGA) formalism is adopted to treat the electronic exchange and correlation effects, as described by Perdew-Burke-Ernzerhof (PBE) [30]. The plane wave basis set with the kinetic energy cut-off of 35 Ry is used for the expansion of the ground state electronic wave functions. The plane waves are chosen to have a periodicity compatible with the periodic boundary conditions of the simulating cell. The supercell dimensions are kept fixed during the relaxation.

We have used calculated value of the lattice constant ($a = 2.46 \overset{o}{A}$), which overlaps with the experimental value [31], obtained from our convergence tests. The adatom graphene system is modeled using single adatom in 2×2, 3×3, and 4×4 supercells of graphene containing 8, 18 and 32 number of carbon atoms. In this work, the adsorption of single Pt atom on graphene is performed at three different high symmetry sites, top (T), hollow (H) and bridge (B). For each adsorption site of the adatom-graphene system, the adatom is relaxed along the z-direction and the C atoms on graphene in all x, y, and z directions. To estimate the binding energy of adatom (Pt), the calculations for the isolated Pt, graphene and adatom-graphene are performed within the identical supercell of graphene. The optimized geometry is obtained with fully relaxed BFGS (Broyden-Fletcher-Goldfarb-Shanno) scheme [32] until the total energy change between two consecutive scf steps becomes less than 10^{-4}Ry and force acting goes below 10^{-3} Ry. The brillioun zone of graphene is sampled in k-space using the Monkhorst-Pack scheme [33] with an appropriate number of k-points. Different sized supercells are considered to see the size effect of the interaction between the isolated adatom and graphene. In order to avoid the interaction between the adatoms at adjacent supercells, vaccum length of supercell was made large enough, i.e. 20Å along z- axis. The detail calculations to study the electronic properties, like density of states (DOS) and electronic band structure of pure graphene and Pt-adsorbed graphene are calculated in 3×3 supercell of graphene and 15×15×1 mesh in k-space.

The adsorption properties of molecular hydrogen are observed on the most stable geometry of platinum decorated 3×3 supercell of graphene. At first, we optimized H_2 molecule and found bond length of 0.75 Å

between two hydrogen atoms. The optimized molecule/s is then placed within the Pt-adatom graphene supercell of height 20Å, very large in comparison to the bond length of H_2, which prevents interaction between two hydrogen molecules at adjacent supercells. The calculations for a large number of molecular hydrogen (up to eight), with in the limit of computational power, has been covered in this study to observe the desirable binding energy and hydrogen storage capacity.

3. Results and Discussion

In the present work, we study the adsorption properties of single Pt on different symmetry sites of 2×2, 3×3, and 4×4 supercells of pure graphene and also present the binding strength/geometry of a number of hydrogen molecules on its preferred geometry.

A. Binding energy and geometry

The Binding energy (ΔE) of adatom on graphene is defined as,

$$\Delta E = E_A + E_G - E_{GA}$$

where, E_{GA}, E_G and E_A are the values of energy of adatom-graphene, pure graphene and an isolated adatom in 3×3 supercell of graphene. Out of the three adsorption sites (H, B and T) considered in present calculations, the configuration with the highest binding energy is defined as the most favored one.

The adatom height (h) is defined as the difference in z coordinates of adatom and the average of the z coordinates of the carbon atoms in the graphene layer. We have also calculated the distance d_{Ac} between the adatom and its nearest carbon atom. The adsorption of adatom on graphene produces a distortion (dz), which is quantified by computing the maximum deviation of C atoms along z-direction from their average positions in pristine graphene. The distortion of the graphene layer upon the adsorption of adatom is also calculated in terms of change in dihedral angles.

Table 1. The binding energy E_b, adatom height h and the nearest carbon distance d_{Ac} for adatom (Pt) in 2×2, 3×3 and 4×4 supercells of graphene are noted. Further, deformation produced in graphene layer due to adsorption of adatom is quantified in terms of distortion along z-direction (dz).

Size of graphene supercell	Adsorption site	Binding Energy (E_b,eV)	Height of Pt atom (h, Å)	Distance of nearest carbon (d_{Ac}, Å)	Distortion (dz, Å)
2×2	H	1.087	2.12	2.48	0.09
	B	1.175	2.09	2.12	0.11
	T	1.089	2.13	2.55	0.09
3×3	H	1.305	1.95	2.41	0.02
	B	2.022	2.15	2.10	0.17
	T	1.905	2.16	2.03	0.01
4×4	H	1.317	1.95	2.40	0.03
	B	2.048	2.20	2.10	0.22
	T	1.917	2.20	2.03	0.16

Table (1) shows that the adsorption of Platinum atom on different sites of pure graphene sheet is feasible. The table also reveals the most favored site for Pt as bridge site with the highest binding energy (E_b). The binding energy seems to increase on increasing the computed graphene size. However, the increment in E_b is nominal for 4×4 supercell with reference to 3×3, and this helps to conclude that size effect of graphene beyond 3×3 does not alter the quality of calculations. Taking care of size effect information and computational cost for bigger system, we consider 3×3 supercell for further calculations.

The distortion in the graphene plane due to the adsorption of adatom is observed maximum at the bridge site. This correlates the direct relationship of distortion with binding energy. The distortion can also be measured in terms of change in bond length, bond angle and dihedral angle. In case of 3×3 graphene sheet, maximum change in bond length, bond angle and dihedral angle are observed as 0.02Å, 0.9^o and 12.07^o from their initial values 1.42 Å, 120^o and 0^o, respectively.

B. Electronic structures

We have computed the electronic density of states (DOS) and band structures of pure graphene and adatom graphene. The Kohn-Sham DOS is computed for adatom at the most favorable (B) site of the 3×3 graphene supercell using 15×15×1 Gamma centered Brillouin zone-sampling. The energy eigen values are smeared by 'Marzari-Vanderbilt' smearing [35] of width 0.001 Ry.

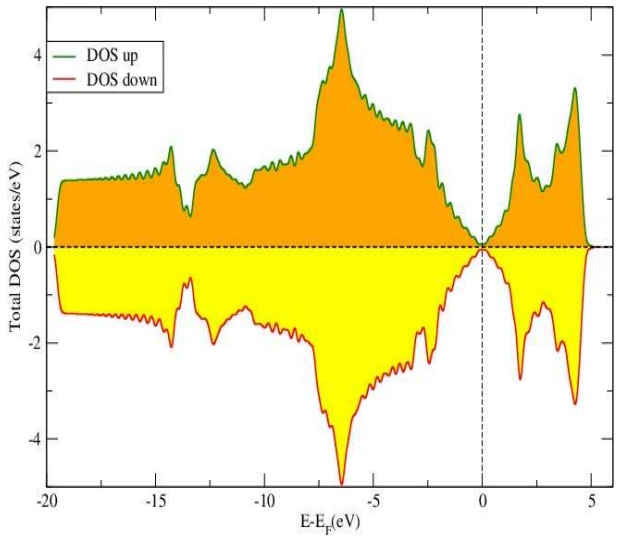

Fig.1 (a)

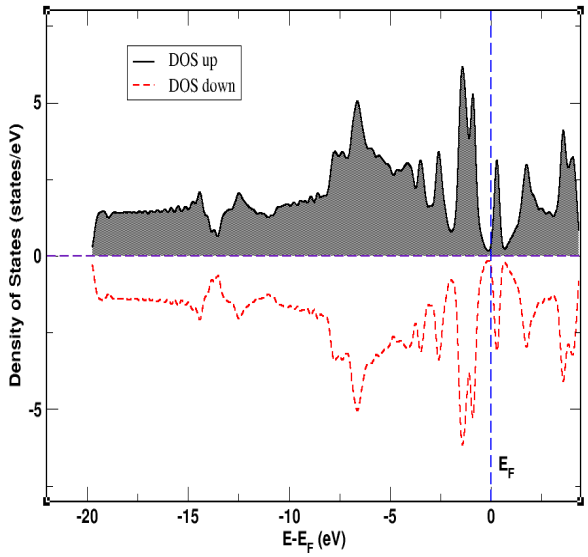

Fig.1 (b)

Figure 1: Plot of density of states for pure graphene (a) and Pt adsorbed graphene (b). The DOS is plotted assuming fermi level as the reference.

The spin up and spin down calculations of pure graphene are plotted by assuming Fermi energy as reference level (Fig. 1a). The Dirac point, where DOS is nearly equal to zero, lies at the Fermi level, and approves that the valence and conduction band meet at that point with zero band gap. The identical density of states for spin up and spin down in the figure approves the non magnetic nature of pure graphene.

From Fig. (1b) it is seen that Fermi level of adatom graphene again appears to remain at the Dirac point. On the other hands, DOS of adatom graphene system has been modified near the Fermi level. The contribution of different Pt orbitals in the DOS of Pt adatom system is shown in Fig. 2.

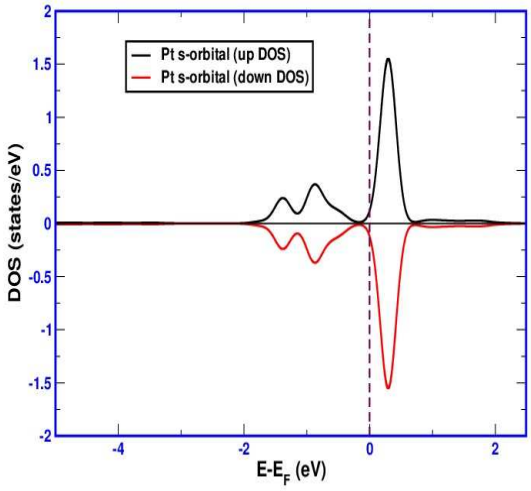

Fig. 2 (a)

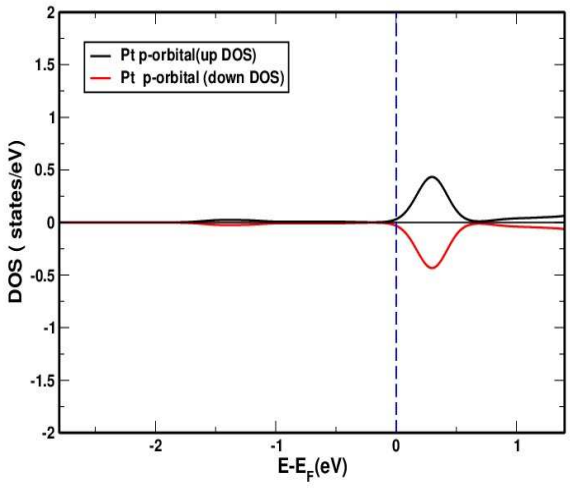

Fig. 2 (b)

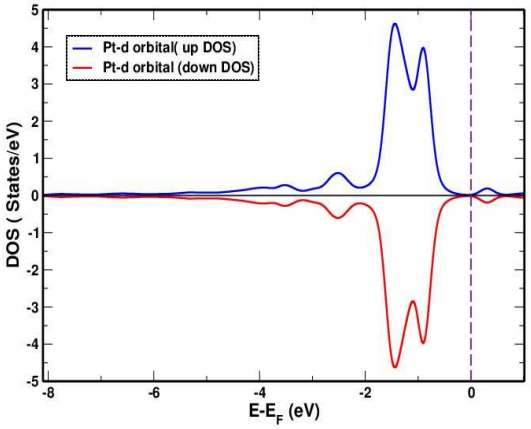

Fig. 2(c)

Figure 2: The projected densityof states (PDOS) for spin up and spin down of s (a), p (b), and d (c) orbitals of Pt, an adatom on graphene.

They show the different orbital's contribution on the DOS of pristine graphene.

The band structure of pure graphene exhibits its unique feature showing zero band gap at Fermi level. The bands meet at a point in Fermi level (observed at -2.351 eV) and form a conical structure, which are known as Dirac point and Dirac cone respectively (Fig. 3a).

The interaction of the adatom with Π and Π* states of the carbon atoms in graphene, however, breaks the symmetry of graphene and band gap occurs at the Fermi level. New bands originating from Pt modify the band structure of pure graphene and disclose a band gap of 1.10 eV in adatom graphene. This change in band gap from zero in pure graphene to 1.10 eV in Pt-added graphene shows the potential use of the material for practical applications.

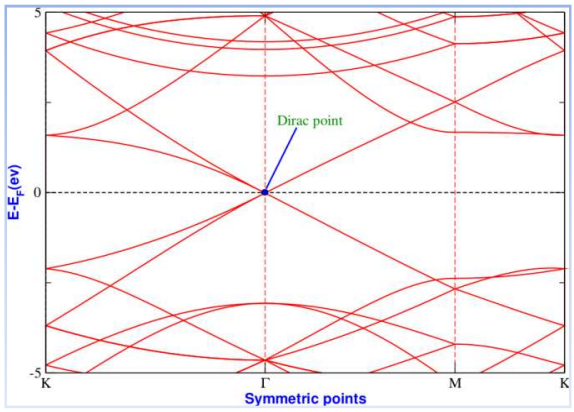

Fig. 3(a)

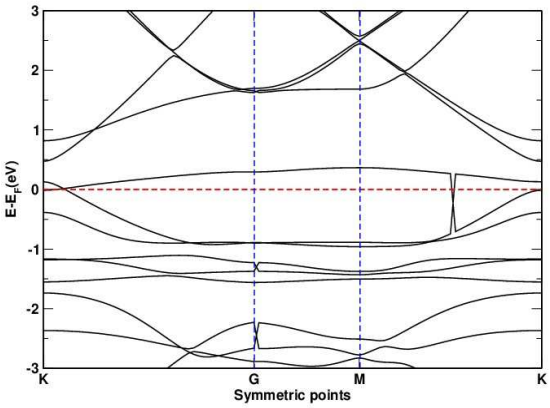

Fig. 3(b)

Figure 3: Band structure of 3×3×3 supercell of pure graphene (a) and Pt-adsorbed graphene (b) along K-Γ- M-K path of irreducible Brillouin zone.

C. Charge transfer

Charge transfer, an ambiguous quantity [16, 17], is an important feature of adatom-graphene interaction in which transfer of electronic charge takes place between the adatom and graphene. In this section, we discuss and quantify the charge transfer due to the adsorption of adatom on bridge site of 3×3 graphene supercell, which we believe an essential part to study the nature of bonding between the interactive materials. By keeping in mind that the magnitude of charge transfer is highly method dependent and difficult to quantify as an absolute value, we have used one of the algorithms followed by previous studies [15], where we integrate differences in electronic charge density in planer basis.

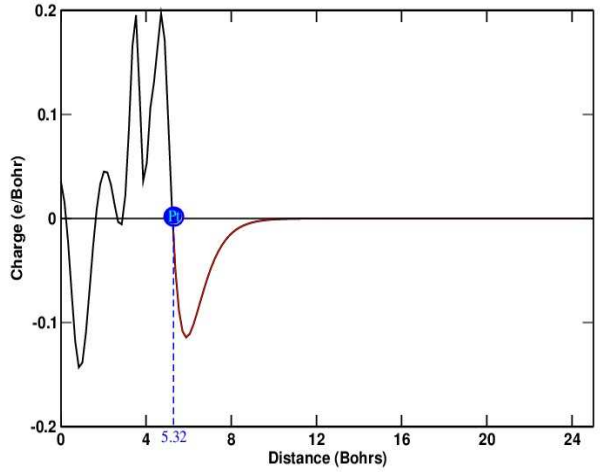

With the help of optimized structures, the charge densities for pure graphene layer, isolated adatom, and adatom graphene are calculated. The difference in charge-density is then defined as

$$\Delta\rho(r) = \rho_{AG}(r) - \rho_A(r) - \rho_G(r)$$

where $\rho_{AG}(r)$, $\rho_A(r)$ and $\rho_G(r)$ are the charge densities of the adatom-graphene, an isolated adatom, and graphene respectively, calculated in the same positions of the supercell as done for adatom-graphene calculations.

Figure 4: Planner averaged electron charge difference for Pt on graphene at B site as a function of position along z-direction. The vertical line at z=0 represents the position of graphene sheet and the line at z = 5.32 Bohr indicates Rcut. The integration between the region z=0 and z=5.32 Bohr quantifies the charge transfer.

Figure (4) shows the planar averaged linear charge density difference as a function of z, along the height of supercell, for Pt on B-site of graphene. The figure implies the position of planar graphene sheet and adatom (Pt) at z = 0 and 5.32 Bohr, respectively. Positive difference in electron density towards the region of graphene sheet and negative towards the adatom illustrates the transfer of electronic charge from adatom to graphene.

To calculate the charge transfer using the linear charge density difference, the region of the space belonging to graphene and/or adatom must be specified. As similar to the concept used by Chan et al., [15], an adsorbate-substrate cutoff distance R_{cut} is defined as the distance from the graphene plane to the point between the plane and the adatom at which charge accumulation changes to charge depletion. In the Fig. (4) the region with $z < R_{cut}$ is assigned to the substrate and the region with $z > R_{cut}$ is assigned to the adatom. The charge transfer is obtained by the integral of linear charge density difference in the substrate region, and the quantity in case of Pt adatom graphene has been found as 0.18e. Higher the value of charge transfer may cause more impacts on the electronic structure and therefore on the catalytic activities of the system.

D. Adsorption of hydrogen molecule/s on Pt adsorbed graphene

We have also performed the first-principles calculations to study the adsorption of hydrogen molecule/s in Pt decorated graphene. The system is modeled by allowing the adsorption of hydrogen molecule/s from one up to maximum eight in number on a single Pt decorated 3×3 graphene supercell. The binding energy (ΔE) of H2 molecule is then calculated using the formula,

$$\Delta E = E_{AG} + E_{H2} - E_{AGH}$$

where E_{AGH} is the energy of the system containing graphene, adatom and H2 molecules, E_{AG} is the energy of the Pt-graphene system and E_{H2} is the energy of the H2 molecule. Furthermore, binding energy/H2 molecule is calculated as,

$$B.E/H2 = \Delta E/N,$$ with N as the number of the hydrogen molecules.

Figure (5) represents the optimized structures for the adsorption of hydrogen molecule/s on Pt decorated graphene system. The figures show that two hydrogen molecules dissociate into atomic hydrogen and a complex, due to interaction with the adatom. Most of the H2 molecules in the larger systems seem to be attracted by long-range dispersion forces.

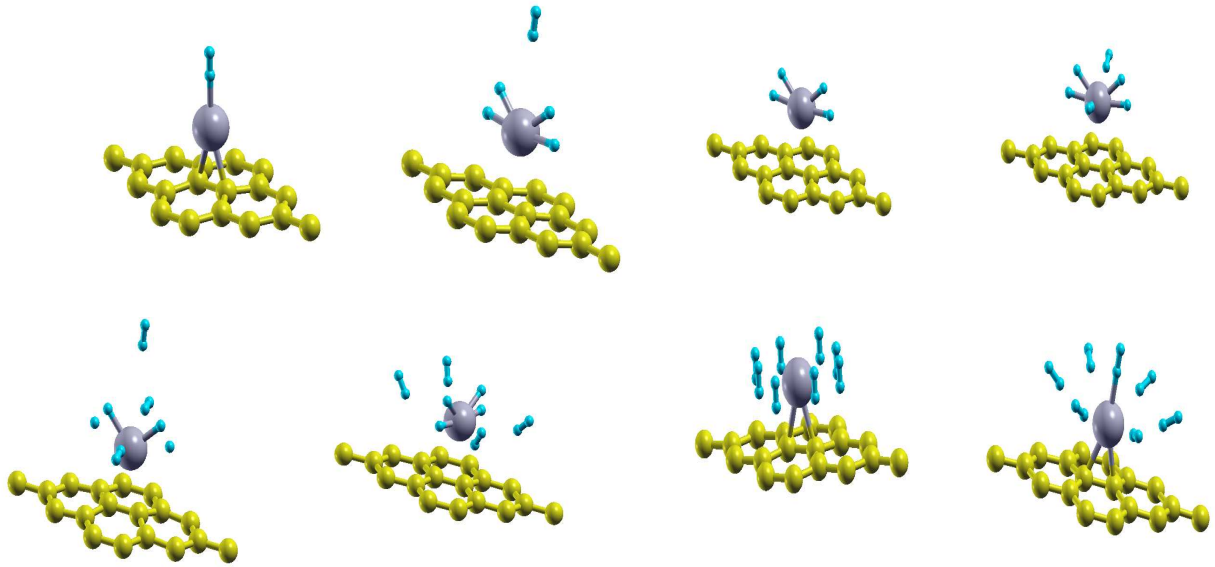

Figure 5: Optimized geometries for the adsorption of H2 in Pt-decorated graphene system.

The variation of the binding energy per H_2 molecule with the number of H_2 molecules adsorbed on Pt-decorated graphene is shown in figure (6). Table (2) presents the observed values of energy of total system, binding energy of H_2 molecules and binding energy per H_2 molecule. It can be seen that the observed binding energy per H_2 molecule decreases with increasing the number of adsorbed hydrogen molecules. When a single hydrogen molecule is adsorbed in Pt-graphene system, the binding energy for H_2 molecule is found 1.84eV. The decreasing pattern of the binding energy per hydrogen molecule, as seen in Fig. 6, for the adsorption of one to eight adsorbed H_2 molecules goes through the range of 1.84 eV to 0.13 eV. The binding energy values per hydrogen molecule from this work meet the U.S. DoE (Department of Energy) target (0.2eV-0.7eV) [36].

Table 2: The binding energy of hydrogen molecules (Eb) and binding energy per H2 molecule (Eb/H2), for the adsorption of H2 molecules in Pt decorated graphene are presented.

Number of H_2 molecule	Binding Energy (eV)	Binding Energy/H2 (eV)
1	0.415	1.847
2	0.914	0.957
3	1.957	0.652
4	1.937	0.484
5	1.985	0.397
6	2.076	0.346
7	1.137	0.162
8	0.904	0.134

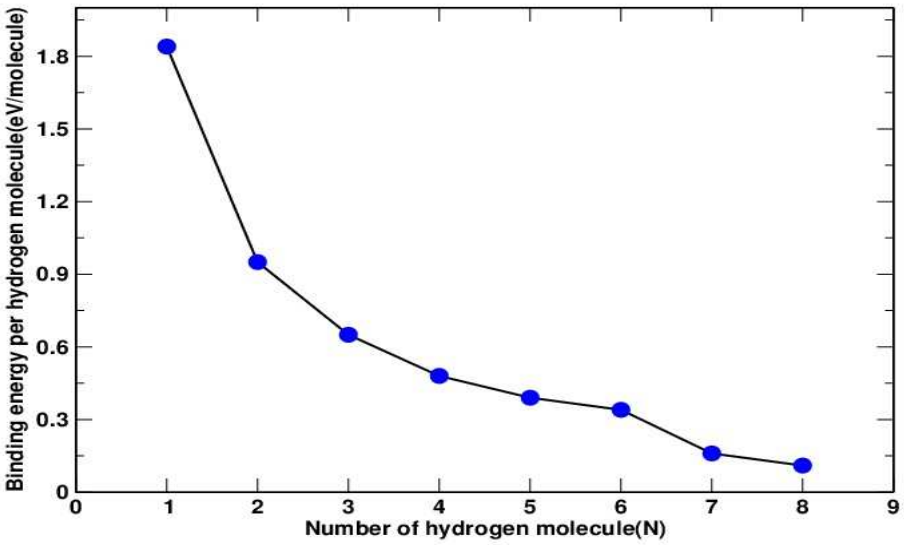

Figure 6: Variation of binding energy per H2 molecule with the number of hydrogen molecule adsorbed in platinum adatom graphene.

One of the major purposes of this study (adsorption of hydrogen molecules on graphene) is to explore the possibility of the gaseous storage at operating conditions. If we compare the strength by which H2 are bound in pure and adatom graphene system, the maximum possible binding energy per H2 molecule is enhanced remarkably in adatom (Pt) graphene (1.84eV) over the pure graphene (~ 0.07 eV). The hydrogen storage capacity of single Pt decorated graphene for the adsorption of 8 H2 molecules is 3.74 wt % per substrate, comparing to the DoE target (around 6 wt %) [9], for the practical applications. The estimated results display the potential application of Pt decorated graphene in hydrogen gas storage material.

4. Conclusion and Concluding remarks

We studied the structural and electronic properties of pure graphene and platinum adsorped graphene systems. Using the estimated values of binding energies of Platinum at three high symmetry sites (H, B and T) of 3×3×3 graphene supercell, it is found that the bridge site is energetically favourable with its magnitude 2.022 eV. The adsorption of adatoms on the bridge site of the graphene changes some of the graphene sp^2 like orbital character to a more covalently reactive sp^3 like character, which is accounted by calculating the deformation on graphene sheet. A small band gap of 1.10eV has been noticed in band structure calculations of Pt-added graphene over the zero band gap pure graphene, which causes the breaking of symmetry of the graphene.

We have also studied the adsorption of the hydrogen molecules on Pt-decorated graphene in order to investigate its hydrogen storage capacity. The binding energy per H2 molecule due to adsorption of one to eight number of hydrogen molecules on Pt adatom graphene ranges within 1.847 eV to 0.134 eV, where its value decreases on increasing the number of adsorbed hydrogens. Within the limit of our calculations, the maximum hydrogen storage capacity of single Pt decorated graphene for 8 H2 molecules is found 3.72 wt %. The results we discussed in this paper, in general, are progressive and interesting to move towards the US DoE criteria (around 6 wt %) for the practical applications.

We intend to extend this work to see the redistribution of charge density while adsorbing adatom and gaseous molecules on graphene. Adsorption of multiple Pt atoms or/and Pt-dimers and also more hydrogen molecules may enhance wt % of hydrogen and overall quality of the material.

Acknowledgments

We acknowledge the partial support from *The Abdus Salam* International Centre for Theoretical Physics (ICTP) through Office of External Activities within NET-56 project. We also extend our gratitude to S. Narasimhan and K. Ulman for their valuable suggestions and inspiration to work in this area.

References

[1] J. W. McClure, Phys. Rev., 104 (1956) 666.

[2] A. K. Geim, K. S. Novoselov, Nat. Mater., 6 (2007) 183.

[3] Y. Zhang, Y. W. Tan, H. L. Stormer, P. Kim, Nature, 438 (2005) 201.

[4] F. Schedin, A. K. Geim, S. V. Morozov, E. W. Hill, P. Blake, M. I. Katsnelson, K. S. Novoselov, Nat. Mater., 6 (2007) 652.

[5] M. Y. Han, B. Oezyilmaz, Y. Zhang, and P. Kim, Phys. Rev. Lett., 98 (2007) 206805.

[6] C. Lee, X. Wei, J. W. Kysar, J. Hone, Science, 321 (2008) 385.

[7] K. S. Novoselov, A. K. Geim, S. V. Morozov, D. Jiang, M. I. Katsnelson, I. V. Grigorieva, S. V. Dubonos, A. A. Firsov, Science, 306 (2004) 666.

[8] Y. Miura, H. Kasai, W. Dino, H. Nakanishi, T. Sugimour, J. Appl. Phys., 93 (2003) 3395.
[9] E. Durgun, S. Ciraci, Y. Yildirim, Phys. Rev. B, 77 (2008) 085405.
[10] J. J. Palacios, J. F. Rossier, L. Brey, Phys. Rev. B, 77 (2008) 195428.
[11] K. Nakada, M. Fujita, G. Dresselhaus, M. S. Dresselhaus, Phys. Rev. B, 54 (1996) 17954.
[12] V. C. P. Medeiros and F. de B. Mota, J. S. A. Mascarenhas, M. C. C. Castilh, Nanotechnology, 21 (2010) 115701.
[13] H. Johll, H. C. Kang, Phys. Rev. B, 79 (2009) 245416.
[14] R. Thapa, D. Sen, M. K. Mitra, K. K. Chattopadhyay, Physica B, 406 (2011) 368.
[15] K. T. Chan, J. B. Neaton, M. L. Cohen, Phys. Rev. B, 77 (2008) 235430.
[16] X. Lui, C. Z. Wang, Y. X. Yao, W. C. Lu, M. Hupalo, M. C. Tringides, K.M. Ho, Phys. Rev. B, 83 (2011) 235411.
[17] R. E. Morris, P. S Wheatley, Angew. Chem. Int. Ed., 47 (2008) 4966.
[18] R. Coontz, B. Hanson, Science, 305 (2004) 957.
[19] A. C. Dillon, K. M. Jones, T. A. Bekkedahl, C. H. Kiang, D. S. Bethune, M. J. Heben, Nature, 386 (1997) 377.
[20] J. S. Arellano, L. M. Molina, A. Rubio, J. A. Alonso, J. Chem. Phys., 112 (2000) 8114.
[21] K. Tada S. Furuya, K. Watanabe, Phys. Rev. B, 63 (2001) 155405.
[22] S. P. Chan, G. Chen, X. G. Gong, Z. F. Liu, Phys. Rev. Lett., 87 (2001) 205502.
[23] Y. Zhao, Y. H. Kim, A. C. Dillion, M.J. Heben, S. B. Zhang, Phys. Rev. Lett., 94 (2005) 155504.
[24] S. Dag, Y. Ozturk, S. Ciraci, T. Yildirim, Phys. Rev. B, 72 (2005) 155404.
[25] T. Yildirim, S. ciraci, Phys. Rev. Lett., 94 (2005) 175501.
[26] P. Hohenberg, W. Kohn, Phys. Rev. B, 136 (1964) 864.
[27] W. Kohn, L. J. Sahm, Phys. Rev., 140 (1965) 1133.
[28] J. Klimes, A. Michaelides, J. Chem. Phys., 137 (2012) 120901.
[29] P. Giannozzi et al., J. Phys.: Condens. Matter, 21 (2009) 395502.
[30] J. P. Perdew, K. Burke, M. Ernzerhof, Phy. Rev., 77 (1996) 3865 .
[31] A. H. Castro Neto, Physics World, 19 (2006) 33.
[32] R. Fletcher, Practical Methods of Optimization, Wiley, New York, 1987.
[33] J. H. Monkhorst, D. J. Pack, Phys. Rev. B, 16 (1977) 1748.
[34] Y. Kyun Kwon, Journal of Korean Physical Society, 57 (2010) 778.
[35] N. Marzari, D. Vanderbilt, A. de Vita, M. C. Payne, Phys. Rev. Lett., 82 (1999) 3296.
[36] J. G. Zhou, Q. L. Willians, J. Nano Research, 15 (2011) 29.